

Translational and Bond-Orientational Order in the Vortex Lattice of the High- T_c Superconductor $\text{Bi}_{2.1}\text{Sr}_{1.9}\text{Ca}_{0.9}\text{Cu}_2\text{O}_{8+\delta}$

D. G. Grier, C. A. Murray, C. A. Bolle,^(a) P. L. Gammel, and D. J. Bishop
AT&T Bell Laboratories, Murray Hill, New Jersey 07974

D. B. Mitzi^(b) and A. Kapitulnik
Stanford University, Stanford, California 94305
 (Received 28 January 1991)

We have investigated the microscopic ordering of the flux lattice in the mixed state of $\text{Bi}_{2.1}\text{Sr}_{1.9}\text{Ca}_{0.9}\text{Cu}_2\text{O}_{8+\delta}$ near H_{c1} by image analysis of Bitter-decorated samples. We observe a dramatic transition from strong isotropic disorder to hexatic order with increasing magnetic field. This transition occurs at a lower applied magnetic field for samples which are annealed in oxygen.

PACS numbers: 74.60.Ge, 74.70.Vy

Layered copper-oxide superconductors have a combination of properties not seen in conventional type-II superconducting materials which include short superconducting coherence lengths, long magnetic penetration depths, very high mass anisotropies, and high critical temperatures. The resulting rich and novel phenomenology has sparked considerable experimental and theoretical effort. One area which has received attention is the nature of the ordering of the magnetic-flux lattice in the mixed state.¹ Measurements of bulk properties such as mechanical dissipation,² transport,³ magnetization,^{4,5} and muon spin resonance⁶ have been interpreted in light of the various predicted phase diagrams which include exotic new ideas about the vortex lattice including flux melting,^{2,7,8} thermally induced entanglement of vortices,^{7,9-12} weak-pinning-induced elastic deformations,^{8,13,14} and strong-pinning-induced disorder.^{11,15} However, such measurements do not probe the microscopic order of the flux lattice which not only differentiates among the proposed configurations, but also exposes the relevant physics of vortex pinning and entanglement.

In this Letter, we report observations of the development of long-range translational and bond-orientational microscopic order in the flux lattice of single-crystal $\text{Bi}_{2.1}\text{Sr}_{1.9}\text{Ca}_{0.9}\text{Cu}_2\text{O}_{8+\delta}$ as a function of applied magnetic fields. We observe an abrupt transition from strong isotropic disorder to a phase with hexatic order. For oxygen-annealed samples, this transition shifts to significantly lower fields.

Our single-crystal Bi-Sr-Ca-Cu-O (2:2:1:2) samples were prepared with a directional solidification technique described elsewhere.¹⁶ Typically, the crystals are rectangular slabs roughly 1 mm wide and 5–30 μm thick with the c axis aligned along the short direction. Some samples were subsequently annealed at 600°C in 1 atm of oxygen for 24 h and then quenched to room temperature, while the rest were examined as made. Magnetization measurements of the as-made samples in an ambient field of 0.5 Oe indicate homogeneous bulk superconduc-

tivity with onset at $T_c = 88.5$ K and a transition width (10%–90%) of 5 K. The annealed samples have an onset temperature of 86 K with a transition width of 2 K. X-ray diffraction shows that the lattice spacing along the c axis shrinks from 30.89(1) to 30.80(1) Å after annealing, while the a and b spacings remain constant at 5.413(2) and 5.411(3) Å, respectively. High-resolution x-ray photoemission spectroscopy of the O_{1s} core levels shows that additional oxygen introduced by oxygen annealing not only fills oxygen vacancies in the Bi-O plane but also may enter the lattice at other points.¹⁷ Despite this structural change, the measured room-temperature resistivity anisotropy¹⁸ of our samples changes by less than 10% with annealing, suggesting that oxygen annealing does not appreciably decrease the carrier mass anisotropy $\Gamma = (m_c/m_a)^{1/2}$. Torque magnetometry¹⁹ indicates $\Gamma = 55$ for as-made samples. Muon spin relaxation²⁰ indicates that the a - b in-plane penetration depth is approximately $\lambda_{\parallel} \approx 0.30$ μm . Assuming a superconducting coherence length of $\xi \approx 15$ Å, the Ginzburg-Landau parameter is $\kappa = \lambda_{\parallel}/\xi \approx 200$.

Twenty specimens cleaved in air along the Bi double layer were cooled immediately to 4.2 K in vacuum with magnetic fields ranging from 5 to 100 G applied normal to the superconducting a - b planes. Flux lines trapped in the samples were then located using the Bitter-decoration technique.²¹ It is important to realize that these field-cooled decoration experiments do not measure the equilibrium configuration of the vortices at 5 K where the decoration takes place, but instead a configuration quenched in at a higher temperature, $T_f(H)$, where the topology of the flux lattice becomes fixed despite thermal motion of individual vortices. At present there are no measurements of $T_f(H)$, although previous decoration experiments have shown appreciable motion of the flux lines at 15 K.²²

We have shown previously²³ for Y-Ba-Cu-O that the vortex density is $n_0 = H/\phi_0$ to within experimental error. We find this to be true for the Bi-Sr-Ca-Cu-O samples as well. For this study, we digitized 42 scanning-

electron-microscopy photographs of Bitter decorations using a video frame grabber at a resolution of 512 by 480 pixels and a dynamic range of 256 gray levels. Two or three pictures were taken near the center of each sample from regions separated by more than $500 \mu\text{m}$. A typical digitized image contains approximately 4000 decoration clusters separated by approximately 8 pixels. The locations of the clusters were then determined to 1 pixel accuracy using an image-processing technique described previously.²⁴ Gradients in the vortex density across images were determined to be less than 0.5%. Experimental uncertainty in vortex location arises both because of the irregular shapes of some clusters and also because of the inherent difficulty in placing a triangular lattice in registry with a square grid.

Figures 1(a), 1(b), and 1(c) show Delaunay triangulations²⁵ for samples decorated at 69, 23, and 8 G, respectively. Each vortex core is represented by a vertex in the triangulation, with bonds drawn to all nearest-neighbor

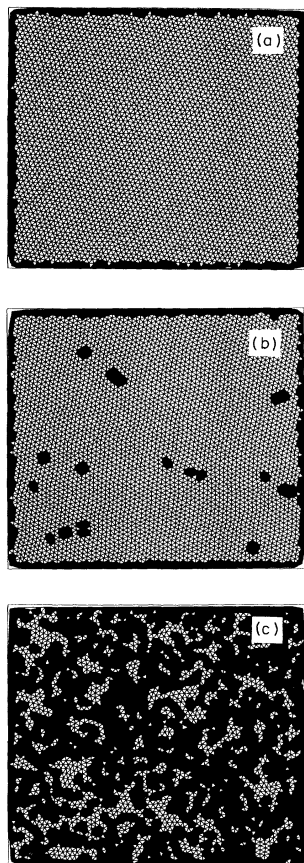


FIG. 1. (a)–(c) Delaunay triangulations for image-processed scanning electron micrographs of Bitter-decorated oxygen-annealed Bi-Sr-Ca-Cu-O cooled to 4.2 K in magnetic fields of 69, 23, and 8 G, respectively. The fields of view are (a) $27 \times 25 \mu\text{m}^2$, (b) $48 \times 45 \mu\text{m}^2$, and (c) $72 \times 68 \mu\text{m}^2$. Shaded triangles adjoin vertices which are not sixfold coordinated.

vortices. Triangles bordering topological defects such as disclinations (nonsixfold coordinated vortices) and edge dislocations (fivefold to sevenfold disclination pairs) in the vortex lattice are shaded. At an applied field of 8 G, Fig. 1(c), the vortex density measured from the photographs is $n_0 = 0.48 \pm 0.04 \mu\text{m}^{-2}$ and the vortex lattice is thoroughly disordered. The fraction of disclination sites f_d is 0.26. At 11 G, $n_0 = 0.60 \pm 0.04 \mu\text{m}^{-2}$, much of the disorder abruptly vanishes ($f_d = 0.07$), leaving only small concentrations of bound and unbound edge dislocations piercing the sample surface. The concentration of lattice defects continues to decrease gradually with increasing applied field as shown in Figs. 1(b) and 1(a), until at $n_0 = 3.57 \pm 0.04 \mu\text{m}^{-2}$ (69 G), we readily find defect-free regions extending beyond the experimental field of view ($f_d < 2 \times 10^{-4}$).

To further elucidate the development of long-range order in the vortex lattice, we have calculated the bond-orientational and translational correlation functions for

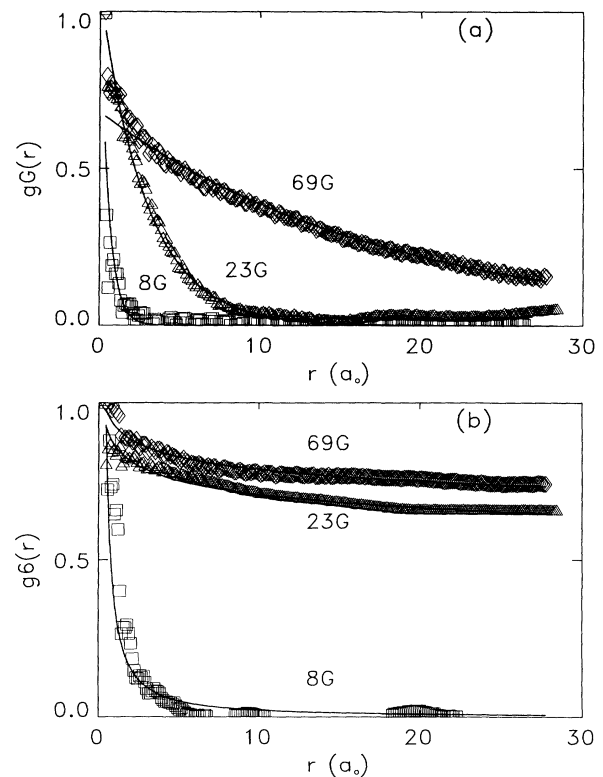


FIG. 2. (a) Translational correlation functions $g_G(r)$ calculated for the vortex locations in Figs. 1(a)–1(c), in units of nearest-neighbor spacings. Diamonds correspond to the 69-G sample, triangles to 23 G, and squares to 8 G. Solid lines are fits by the form $g_G(r) = A \exp(-r/\xi_G)$. (b) Bond-orientational correlation functions $g_6(r)$ calculated for the triangulations in Figs. 1(a)–1(c), in units of nearest-neighbor spacings a_0 . Solid lines are fits by the form $g_6(r) = A \times (r/a_0)^{-n_6}$.

the measured sets of vortex locations. The translational correlation function²⁶ $g_{\mathbf{G}}(r)$ is calculated from the order parameter for each site j : $\psi_{\mathbf{G}}(\mathbf{r}_j) = \exp(i\mathbf{G} \cdot \mathbf{r}_j)$, where \mathbf{G} is a first reciprocal-lattice vector obtained from the power spectrum of the vortex locations. Figure 2(a) shows $g_{\mathbf{G}}(r)$ for the images in Fig. 1. We have fitted the correlation functions with a simple exponential decay²⁷ $g_{\mathbf{G}}(r) \sim \exp(-r/\xi_{\mathbf{G}})$ with correlation lengths $\xi_{\mathbf{G}}$ ranging from $1a_0$ for the 8-G sample to approximately $20a_0$ in the 69-G example. The longest correlation length obtainable with our imaging system is approximately $50a_0$, as determined by performing the same analysis on digitized perfect hexagonal lattices with random displacements of points by up to 2 pixels as would be expected from both registry and digitization errors. Figure 3(a) shows the range of correlation lengths measured for the least disordered spot on each sample with three different choices of \mathbf{G} as a function of applied magnetic field for both annealed and as-made samples. In both cases, the translational order increases monotonically with increasing magnetic field and shows no sign of saturating at our

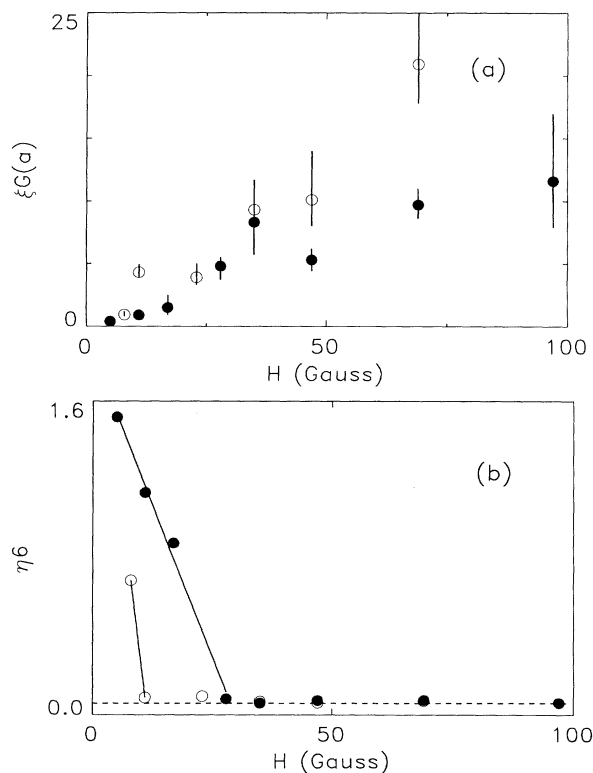


FIG. 3. (a) Translational correlation lengths $\xi_{\mathbf{G}}$ for annealed (open circles) and as-made (solid circles) samples, in units of nearest-neighbor spacings. Error bars represent the range of $\xi_{\mathbf{G}}$ for three different values of \mathbf{G} . (b) Bond-orientational exponents η_6 for annealed (open circles) and as-made (solid circles) samples. The line at $\eta_6 \approx 0.06$ is the limit of our experimental resolution.

highest field. The anisotropy in the vortex lattice measured as the maximum ratio of the magnitudes, $|\mathbf{G}|$, ranged from 3% to 9% which is smaller than the 20% expected²⁸ from the measured effective-mass anisotropy.²⁹ Furthermore, the anisotropy appears to be directed randomly with respect to the underlying crystalline axes.

The sixfold bond-orientational order parameter at vortex location j is defined²⁶ as

$$\psi_6(\mathbf{r}_j) = n_j^{-1} \sum_{k \in \langle nn \rangle_j} \exp(i6\theta_{jk}),$$

where $\langle nn \rangle_j$ is the set of n_j nearest neighbors and θ_{jk} is the angle made by the bond from site j to site k with respect to a fixed axis. The correlation function for this order parameter, $g_6(r)$, is plotted in Fig. 2(b) for the samples at 8, 23, and 69 G. The solid lines are fits by the algebraic form $g_6(r) \sim r^{-\eta_6}$. The 23-G sample has long-range orientational order ($\eta_6 = 0.09$), while its translational order falls off rapidly ($\xi_{\mathbf{G}} \approx 3a_0$). This is the definitive signature of the hexatic phase.²⁶ The 69-G sample has both longer-range translational and orientational order and no topological lattice defects within our sampling area. The exponents η_6 for the samples selected for Fig. 3(a) appear in Fig. 3(b). The dashed line at $\eta_6 \approx 0.06$ shows the limit of our experimental resolution, determined by imaging a perfect hexagonal lattice, below which we can say that a sample has developed long-range orientational order, or $g_6(r) \rightarrow \text{const}$.

For samples with translational correlation lengths in the range $2a_0 < \xi_{\mathbf{G}} < 10a_0$, the measured values of $\xi_{\mathbf{G}}$ and η_6 are consistent with the measured density of free edge dislocations,³⁰ suggesting that topological defects determine the order in this regime. We note that the theories of vortex lattice pinning that include only elastic interactions^{8,13,27,31} do not include the possibility of such topological defects. For samples at higher fields with $10a_0 < \xi_{\mathbf{G}} < 20a_0$, $\xi_{\mathbf{G}}$ is considerably smaller than that expected from the average distance between dislocations and reflects small random lattice displacements.

We see a clear shift of the disorder-hexatic transition from 8 G for the annealed samples to approximately 20 G for the as-made samples³² as shown in Fig. 3.

Theories including both pinning and thermal effects appear consistent with the above observations. Fisher, Fisher, and Huse¹⁴ predict a phase transition between an isotropic disordered flux liquid at low magnetic field (high temperature) and a solid shown to be hexatic⁸ at high field (low temperature) for a system with weak pinning. In the absence of strong pinning, vortex entanglement theories^{7,9-11} predict abrupt transitions between isotropic fluids, hexatic fluids, and solids. In either case, agreement between theory and our experiments would require $T_f(H)$ to decrease dramatically with increasing H .⁵ Elastic theories which do not include topological defects may still apply to this experiment in the range where the separation between free edge dislocations

exceeds the experimental field of view. Indeed, the linear increase of ξ_G with H predicted by Chudnovsky²⁷ using a local elastic theory with random weak pinning is consistent with the trend in Fig. 3(a). This increase is inconsistent with the predictions of nonlocal elastic theories which take thermal softening effects into account.³¹

Strong pinning of entangled vortices may also be responsible for an abrupt transition from strongly pinned disorder near H_{c1} to a regime dominated by thermal fluctuations.¹¹ Theories invoking strong pinning due to surface steps and pits³³ or a distribution of strong-pinning centers in the bulk⁹ predict a transition between ordered and disordered configurations of vortices, but would have to explain the extremely rapid (8 to 11 G) disappearance of disorder which we see at relatively low vortex density. Differentiating among the competing theories requires information on the mobility of vortices as a function of temperature and also on the dependence of flux lattice ordering on sample thickness.

We acknowledge helpful discussions with D. Harshman, D. Huse, S. Martin, D. Nelson, and A. Sudbo. Two of the authors would like to acknowledge support received from AT&T (D.B.M.) and the NSF (A.K.). This work was supported in part by the Joint Services Electronic Program under Grant No. N00014-84-K-0327 and by the Stanford Center for Materials Research through the NSF Department of Materials Research.

^(a)Present address: Instituto Balseiro, 8400 Bariloche, Rio Negro, Argentina.

^(b)Present address: IBM T. J. Watson Research Center, Yorktown Heights, NY 10598.

¹P. L. Gammel, *J. Appl. Phys.* **67**, 4676 (1990).

²P. L. Gammel, L. F. Schneemeyer, J. V. Waszczak, and D. J. Bishop, *Phys. Rev. Lett.* **61**, 1666 (1988).

³R. Koch, V. Foglietti, W. J. Gallagher, G. Koren, A. Gupta, and M. P. A. Fisher, *Phys. Rev. Lett.* **63**, 1511 (1989); T. K. Worthington, F. H. Holtzberg, and C. A. Feild, *Cryogenics* **30**, 417 (1990).

⁴P. H. Kes and C. J. van der Beek, in Proceedings of the ICMC-90 Topical Conference on High-Temperature Superconducting Materials, Garmisch-Partenkirchen, Germany, 9-11 May 1990 (to be published).

⁵L. Lombardo, M. Ng, J. S. Urbach, D. B. Mitzi, and A. Kapitulnik (to be published).

⁶D. R. Harshman, L. F. Schneemeyer, J. V. Waszczak, G. Aeppli, R. J. Cava, B. Batlogg, L. W. Rupp, E. J. Ansaldo, and D. L. Williams, *Phys. Rev. B* **39**, 851 (1989); D. R. Harshman, R. N. Kleiman, M. Inui, G. P. Espinosa, D. B. Mitzi, A. Kapitulnik, T. Pfiz, and D. L. Williams (to be published).

⁷D. R. Nelson, *Phys. Rev. Lett.* **60**, 1973 (1988).

⁸A. Houghton, R. A. Pelcovits, and A. Sudbo, *Phys. Rev. B* **40**, 6763 (1989).

⁹D. R. Nelson and H. S. Seung, *Phys. Rev. B* **39**, 9153 (1989).

¹⁰M. C. Marchetti and D. R. Nelson, *Phys. Rev. B* **40**, 1910

(1990).

¹¹D. R. Nelson and P. LeDoussal (to be published).

¹²S. P. Obukhov and M. Rubinstein, *Phys. Rev. Lett.* **65**, 1279 (1990).

¹³E. M. Chudnovsky, *Phys. Rev. B* **40**, 11 355 (1989).

¹⁴M. P. A. Fisher, *Phys. Rev. Lett.* **62**, 1415 (1989); M. P. A. Fisher, D. Fisher, and D. Huse, *Phys. Rev. B* **43**, 130 (1991).

¹⁵E. H. Brandt, *Phys. Rev. Lett.* **63**, 1106 (1989); *J. Low Temp. Phys.* **64**, 375 (1986); *Phys. Rev. B* **34**, 6514 (1986).

¹⁶D. B. Mitzi, L. W. Lombardo, A. Kapitulnik, S. S. Landerman, and R. D. Jacowitz, *Phys. Rev. B* **41**, 6564 (1990).

¹⁷F. Parmigiani, Z. X. Shen, D. B. Mitzi, I. Lindau, W. E. Spicer, and A. Kapitulnik, *Phys. Rev. B* **43**, 3085 (1991).

¹⁸S. Martin (private communication). Measurements on the (2:2:0:1) materials also suggest that Γ should change by less than a factor of 3. S. Martin, A. T. Fiory, R. M. Fleming, L. F. Schneemeyer, and J. V. Waszczak, *Phys. Rev. B* **41**, 846 (1990). Changes in Γ could conceivably be offset in these measurements by compensating shifts in the scattering time anisotropy.

¹⁹D. E. Farrell, S. Bonham, J. Foster, Y. C. Chang, P. Z. Jiang, K. G. Vandervoort, D. J. Lam, and V. G. Kogan, *Phys. Rev. Lett.* **63**, 782 (1989).

²⁰D. R. Harshman, R. N. Kleiman, M. Inui, G. P. Espinosa, D. B. Mitzi, A. Kapitulnik, T. Pfiz, and D. L. Williams (to be published).

²¹R. P. Huebener, *Magnetic Flux Structures in Superconductors* (Springer-Verlag, New York, 1979), p. 100ff.

²²R. N. Kleiman, P. L. Gammel, L. F. Schneemeyer, J. V. Waszczak, and D. J. Bishop, *Phys. Rev. Lett.* **62**, 2331 (1989). Macroscopic magnetization studies (Ref. 5) show that the density of flux lines, although not necessarily their local arrangement, becomes fixed for samples similar to those in our study, at a temperature T_{irr} very close to T_c ($T_{irr}=0.99T_c$ at $H=5$ G and $T_{irr}=0.90T_c$ at $H=100$ G).

²³P. L. Gammel, D. J. Bishop, G. J. Dolan, J. R. Kwo, C. A. Murray, L. F. Schneemeyer, and J. V. Waszczak, *Phys. Rev. Lett.* **59**, 2593 (1987).

²⁴D. H. Van Winkle and C. A. Murray, *J. Chem. Phys.* **89**, 3885 (1988).

²⁵F. F. Preparata and M. L. Shamos, *Computational Geometry, an Introduction* (Springer-Verlag, New York, 1985); S. Fortune, *Algorithmica* **2**, 153 (1987).

²⁶B. I. Halperin and D. R. Nelson, *Phys. Rev. Lett.* **41**, 121 (1978); D. R. Nelson and B. I. Halperin, *Phys. Rev. B* **19**, 2457 (1979).

²⁷E. M. Chudnovsky, *Phys. Rev. Lett.* **65**, 3060 (1990).

²⁸G. J. Dolan, F. Holtzberg, C. Feild, and T. R. Dinger, *Phys. Rev. Lett.* **62**, 2184 (1989); L. J. Campbell, M. M. Doria, and V. G. Kogan, *Phys. Rev. B* **38**, 2439 (1988).

²⁹S. Martin, A. T. Fiory, R. M. Fleming, L. F. Schneemeyer, and J. V. Waszczak, *Phys. Rev. Lett.* **60**, 2194 (1989).

³⁰D. R. Nelson, M. Rubinstein, and F. Spaepen, *Philos. Mag.* **A 46**, 105 (1982).

³¹A. Houghton, R. A. Pelcovits, and A. Sudbo (to be published), and references therein.

³²The results of this study agree with the previous results obtained on as-made samples at 20 G. C. A. Murray, P. L. Gammel, D. J. Bishop, D. B. Mitzi, and A. Kapitulnik, *Phys. Rev. Lett.* **64**, 2312 (1990).

³³David Huse (private communication).